Journal of Dental Research
2017, Vol. 96(2) 192–199

DOI: 10.1177/0022034516682005
journals.sagepub.com/home/jdr

GelMA-Encapsulated hDPSCs and HUVECs for Dental Pulp Regeneration

A. Khayat[1], N. Monteiro[1], E.E. Smith[1,2], S. Pagni[1], W. Zhang[1], A. Khademhosseini[3], and P.C. Yelick[1,2]

Abstract

Pulpal revascularization is commonly used in the dental clinic to obtain apical closure of immature permanent teeth with thin dentinal walls. Although sometimes successful, stimulating bleeding from the periapical area of the tooth can be challenging and in turn may deleteriously affect tooth root maturation. Our objective here was to define reliable methods to regenerate pulp-like tissues in tooth root segments (RSs). G1 RSs were injected with human dental pulp stem cells (hDPSCs) and human umbilical vein endothelial cells (HUVECs) encapsulated in 5% gelatin methacrylate (GelMA) hydrogel. G2 RSs injected with acellular GelMA alone, and G3 empty RSs were used as controls. White mineral trioxide aggregate was used to seal one end of the tooth root segment, while the other was left open. Samples were cultured in vitro in osteogenic media (OM) for 13 d and then implanted subcutaneously in nude rats for 4 and 8 wk. At least 5 sample replicates were used for each experimental group. Analyses of harvested samples found that robust pulp-like tissues formed in G1, GelMA encapsulated hDPSC/HUVEC-filled RSs, and less cellularized host cell–derived pulp-like tissue was observed in the G2 acellular GelMA and G3 empty RS groups. Of importance, only the G1, hDPSC/HUVEC-encapsulated GelMA constructs formed pulp cells that attached to the inner dentin surface of the RS and infiltrated into the dentin tubules. Immunofluorescent (IF) histochemical analysis showed that GelMA supported hDPSC/HUVEC cell attachment and proliferation and also provided attachment for infiltrating host cells. Human cell-seeded GelMA hydrogels promoted the establishment of well-organized neovasculature formation. In contrast, acellular GelMA and empty RS constructs supported the formation of less organized host-derived vasculature formation. Together, these results identify GelMA hydrogel combined with hDPSC/HUVECs as a promising new clinically relevant pulpal revascularization treatment to regenerate human dental pulp tissues.

Keywords: pulp biology, vascular biology, endodontics, tissue engineering

Introduction

Pulpal revascularization therapy is commonly used on injured teeth to promote continued root development and prevent fracture of thin dentinal walls. The goal of this therapy is to achieve apical closure development similar to that of adjacent teeth, to prevent tooth and supporting bone loss, and to avoid the need for a dental implant (Bansal et al. 2014). Induced bleeding at the tooth apex can be used to activate proliferation and migration of stem cells from the apical papilla (SCAP) into the pulpal space and release of growth factors, including platelet-derived growth factor, which participate in angiogenesis (Shah et al. 2008; Zhujiang and Kim 2016). Unfortunately, insufficient bleeding can result, leading to arrested tooth root development, incomplete closure of the tooth apex, and calcification within the pulpal space (Chen, Chen, et al. 2012).

Several attempts to regenerate the dentin-pulp complex combined cells, including human dental pulp stem cells (hDPSCs), human umbilical vein endothelial cells (HUVECs), and SCAP, with scaffolds such as PuraMatrix (BD Biosciences), nanofibrous gelatin/silica bioactive glass hybrid, collagen, poly-L-lactic acid, and fluorapatite crystal coated with polycaprolactone (Cordeiro et al. 2008; Chueh et al. 2009; Huang et al. 2010; Galler et al. 2011; Qu and Liu 2013; Rosa et al. 2013; Dissanayaka et al. 2014; Guo et al. 2014; Palasuk et al. 2014; Dissanayaka, Hargreaves, et al. 2015). Others used scaffold-free approaches, including cell sheet technologies, and dental stem cell (DSC) aggregates formed on agarose dishes (Syed-Picard et al. 2014; Dissanayaka, Zhu, et al. 2015).

Gelatin methacrylate (GelMA) hydrogels exhibit numerous properties useful for tissue engineering applications, including the following: 1) GelMA is largely composed of denatured collagen and retains arginylglycylaspartic acid (RGD) adhesive domains and matrix metalloproteinase (MMP)–sensitive sites that enhance cell binding and cell-mediated matrix degradation, 2) physical properties of GelMA hydrogels can be tuned by varying GelMA and/or photoinitiator (PI) concentrations; 3) GelMA is suitable for cell encapsulation at 37°C and promotes cell viability and proliferation, and 4) GelMA is relatively inexpensive (Nichol et al. 2010; Hosseini et al. 2012).

[1]Tufts University School of Dental Medicine, Boston, MA, USA
[2]Department of Cell, Molecular, and Developmental Biology, Sackler School of Graduate Biomedical Sciences, Tufts University School of Medicine, Boston, MA, USA
[3]Harvard Medical School, Boston, MA, USA

A supplemental appendix to this article is available online.

Corresponding Author:
P.C. Yelick, 136 Harrison Avenue, M824, Boston, MA 02111, USA.
Email: Pamela.Yelick@tufts.edu

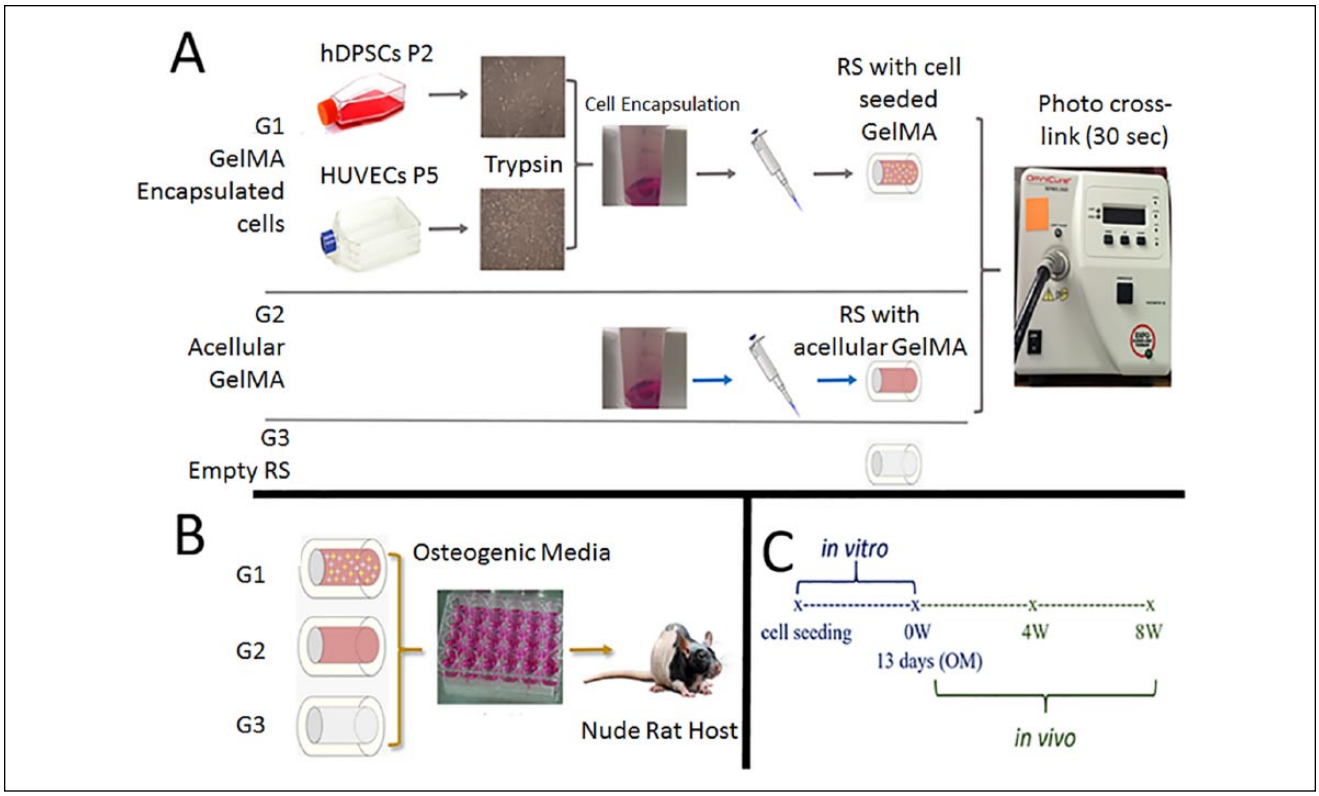

Figure 1. Schematic of study design. (**A**) Gelatin methacrylate (GelMA)–encapsulated human dental pulp stem cell (hDPSC)/human umbilical vein endothelial cell (HUVEC) constructs (G1) consisted of cultured hDPSCs and HUVECs encapsulated in 5% of GelMA, injected into human tooth root segments (RSs), and photo-crosslinked for 30 s. Acellular GelMA constructs (G2) were also injected into RSs and photo-crosslinked for 30 s. Empty RSs (G3) received no treatment. (**B**) Replicate constructs (G1, G2, G3) were cultured in osteogenic media (OM) for 13 d, then implanted subcutaneously for 4 or 8 wk. (**C**) Schematic timeline of the study.

Based on these characteristics, we used GelMA to create 3-dimensional (3D) biomimetic tooth bud models consisting of GelMA-encapsulated dental epithelial (DE) and GelMA-encapsulated dental mesenchymal (DM) cell bilayers, designed to facilitate DE-DM cell interactions, leading to ameloblast and odontoblast differentiation (Smith et al. 2014; Smith et al. 2016). To further this approach, here we examine the use of GelMA hydrogels for pulp tissue regeneration. To our knowledge, this is the first study to validate the use of GelMA-encapsulated hDPSCs/HUVECs for clinically relevant applications for pulpal regeneration.

Materials and Methods

Human Teeth Procurement, Dental Cell Isolation, and In Vitro Expansion

Human teeth extracted for clinically relevant reasons were obtained from the Tufts University School of Dental Medicine and the Back Bay Oral Maxillofacial clinic in Boston, Massachusetts. hDPSCs were isolated from dental pulp obtained from extracted wisdom teeth, as previously published (Zhang et al. 2010). HUVECs (PSC100010; ATCC) were pre-cultured in vascular basal media (VBM) (PCS100030; ATCC) with a vascular endothelial growth factor (VEGF) kit (PCS10004; ATCC), as recommended.

Research Design

Three groups of root segments (RSs) were examined in this study: 1) G1, GelMA-encapsulated hDPSC/HUVEC-filled RSs; 2) G2, acellular GelMA-filled RSs; and 3) G3, empty RS. Briefly, replicate samples were cultured for 13 d in osteogenic media (OM) in vitro. Five replicates of each group were fixed at this time and analyzed using histological and immunohistochemical methods. The remaining RSs were implanted subcutaneously in nude rats and grown for 4 and 8 wk (Fig. 1).

GelMA Preparation

Lyophilized GelMA was fully dissolved in Dulbecco's modified Eagle's medium (DMEM)/F12 media (w/v), and 0.1% of PI (Irgacure2959; Sigma-Aldrich) was added to create a 5% GelMA solution that was filter sterilized using a 0.22-μm filter and stored in the dark until use.

Tooth Root Section Selection Criteria, Disinfection, and Mineral Trioxide Aggregate Placement

Teeth selected from healthy patients aged 15 to 30 y included single and multirooted teeth with type I and V Vertucci root canal configurations. Teeth containing caries, type II to IV Vertucci root canal configuration, calcified canals, or prior root

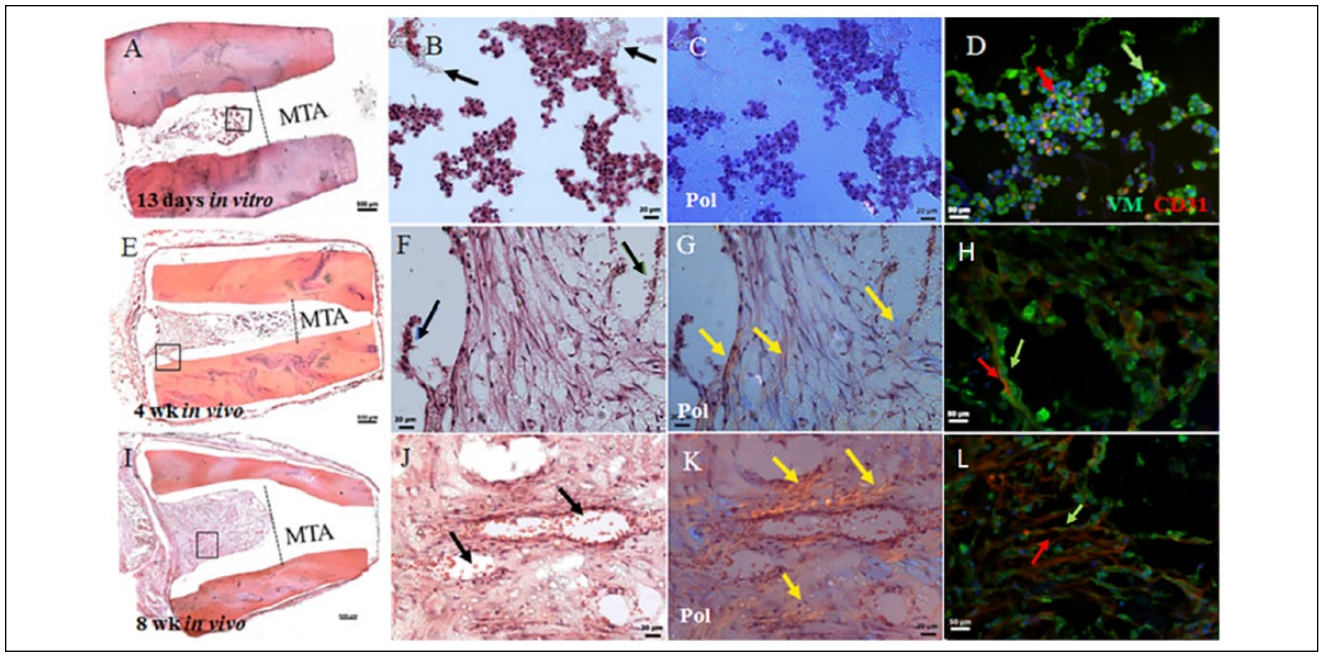

Figure 2. Gelatin methacrylate (GelMA)–encapsulated human dental pulp stem cell (hDPSC)/human umbilical vein endothelial cell (HUVEC) root segment (RS) (G1). (**A**) Sectioned G1 construct after 13 d of in vitro culture showing bioengineered pulp and location of the mineral trioxide aggregate (MTA) plug. (**B**) Enlarged view of boxed area in A showing cellularity of construct and nondegraded GelMA (black arrows). (**C**) Polarized light microscopy (Pol) showed minimal extracellular matrix (ECM) deposition at this time. (**D**) Double immunofluorescence (IF) of CD31-expressing HUVECs (red arrow) and Vimentin (VM)–expressing hDPSCs (green arrow). (**E**) Sectioned 4-wk implanted construct exhibited higher cell density and organization compared with 13 d in vitro. (**F**) Odontoblast-like cells were present at the pulp-dentin interface (blue arrows), and functional neovascularization containing red blood cells was observed (green arrow). (**G**) Pol microscopy showed obvious ECM deposition at 4 wk compared with 13 d of in vitro cultured RS (yellow arrows). (**H**) Double IF showed increased cellularity of both hDPSCs (green arrow) and HUVECS (red arrow). (**I**) The 8-wk in vivo implanted G1 constructs exhibited high cellularity. (**J**) Implant vascularization appeared more distinct compared with 4-wk G1 implants (black arrows). (**K**) Increased collagen deposition was apparent compared with 4-wk in vivo implanted G1 constructs (yellow arrows). (**L**) Double IF revealed high cellularity of hDPSCs and HUVECS. Scale bars: A, E, I = 500 µm; B, C, F, G, J, K= 20 µm; and D, H, L = 50 µm. This figure is available in color online.

canal treatment were excluded. Tooth RSs ~6 mm in length and a 2- to 3-mm orifice width were cut from the coronal and middle third of the roots using sterilized 330 and fissure burs. The pulpal space lumen was enlarged using Gates Glidden sizes 1 and 2, as well as 330 and fissure burs. RSs were treated with EDTA, NaOCL, and phosphate-buffered saline (PBS) washes as described (Galler et al. 2011). To test for microbial contamination, RSs were cultured in DMEM/F12 media at 37°C for 4 d (Galler et al. 2011). White mineral trioxide aggregate (WMTA; ProRoot DENTSPLY Tulsa Dental Specialties) was used to create a plug at one end of each RS to mimic clinical treatment, while the other end was left open.

Cell Preparation and GelMA Encapsulation

A total of 6×10^5 hDPSCs and 6×10^5 HUVECs (1:1) were resuspended in 0.5 mL of filtered 5% GelMA. Approximately 30 µL of GelMA with hDPSCs/HUVECs (~7.0×10^4 cells) or acellular GelMA was injected into RSs and photo-crosslinked via exposure to 9.16-W/cm^2 UV light for 20 s using an Omnicure S2000 (Lumen Dynamics Group).

Tooth Root Implantation and Harvest

All animal procedures were conducted using Tufts University–approved Institutional Animal Care and Use Committee protocols. Implants were placed subcutaneously on the backs of female nude rats aged 4 to 6 wk. All animals survived implantations and exhibited no adverse effects. Replicate RSs were harvested at 4 and 8 wk, fixed in 10% formalin, and decalcified in 10% EDTA at pH 7.0 for 4 mo. Decalcification was monitored weekly by combining 5 mL of the 10% EDTA solution, 1 drop of 1.0 M HCl, and 1 mL of saturated ammonium oxalate. Lack of $CaPO_4$ precipitate formation after 20 min was defined as complete decalcification.

Histological and Immunofluorescent Histochemical Analyses

Samples were prepared and cryosectioned as previously described using a Leica Biosystems cryostat (Zhang et al. 2016). Magic Tape (Cryofilm Type2C; Section-Lab) was used to transfer sections to Superfrost Plus Microscope Slides Precleaned (Fisher Scientific), which were stored at −20°C until use. Slides were hematoxylin and eosin (H&E) stained using standard protocols. Double immunofluorescent (IF) histochemical analysis was performed as previously described (Smith et al. 2016). Primary antibodies included mouse α CD31(1:200, ab187377; Abcam) and rabbit α Vimentin (1:25, bs-0756R; Bioss). Secondary antibodies included goat α mouse (568, 1:50; Invitrogen) and goat α rabbit (488, 1:50; Invitrogen). Mouse α rh-mitochondria (1:25, MAB1273; Millipore Sigma),

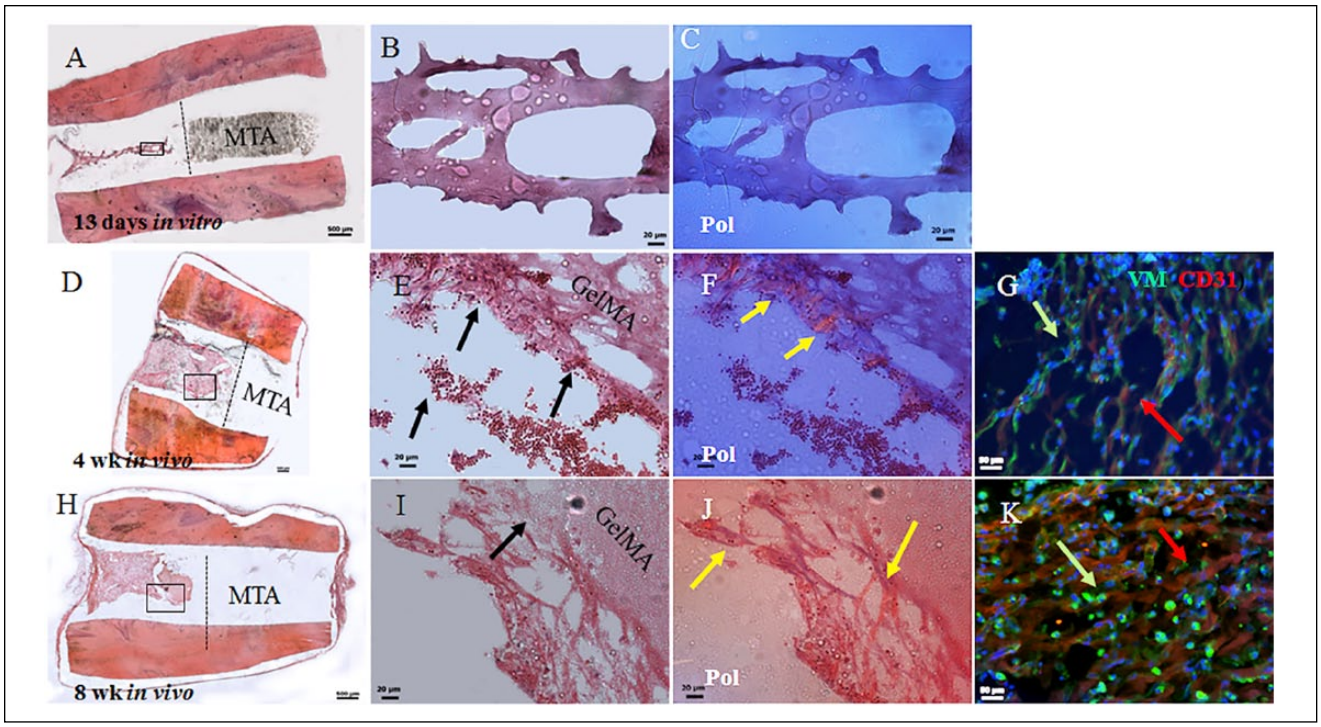

Figure 3. Acellular gelatin methacrylate (GelMA) root segment (RS) constructs (G2). (**A**) Sectioned 13-d in vitro cultured acellular RSs exhibited degraded GelMA and remnant mineral trioxide aggregate (MTA). (**B**) Enlarged boxed area in A shows remnant GelMA. (**C**) Polarized light imaging did not detect organized collagen. (**D**) The 4-wk in vivo G2 implants exhibited increased cellularity compared with 13-d in vitro cultured G2 constructs. (**E**) Enlarged area in D shows host cellularity, attachment to GelMA, and vascularity, including host red blood cells (black arrows). (**F**) Polarized light revealed host cell–derived extracellular matrix (ECM; yellow arrows). (**G**) Double immunofluorescence (IF) revealed host CD31-expressing endothelial and vimentin-expressing mesenchymal cells. (**H**) Sectioned 8-wk implant revealed high cellularity and invading host cells. (**I**) Enlarged boxed area in H revealed nondegraded GelMA that persisted in 8-wk in vivo implanted G2 constructs and host cells (black arrow). (**J**) Polarized light microscopy revealed increased host derived ECM deposition compared with 4-wk in vivo implanted G2 constructs (yellow arrows). (**K**) Double IF revealed CD31-expressing host endothelial cells and Vimentin (VM)–expressing host mesenchymal cells in 4-wk in vivo implanted G2 constructs. Scale bars: A, D, H = 500 μm; B, C, E, F, I, J = 20 μm; and G, K = 50 μm. This figure is available in color online.

which recognizes human cells and does not cross-react with rat cells, was used to discriminate between GelMA-encapsulated hDPSC/HUVECs in G1 constructs and rat host endothelial cells.

Results

(G1) GelMA-Encapsulated Cell Tooth RSs

G1, GelMA-encapsulated hDPSC/HUVEC RSs exhibited cellularized bioengineered pulp-like tissue after 13 d of in vitro culture (Fig. 2A, B). The cellularity of G1 constructs was increased in 4 wk for in vivo implanted constructs (Fig. 2E, F, I, J) and at 8 wk occupied the entire pulpal space not containing mineral trioxide aggregate (MTA). Neovascularization of pulp-like tissue was observed at 4 wk (Fig. 2H). At 8 wk of in vivo implantation, G1 implants showed patent blood vessels filled with host red blood cells (Fig. 2J, arrows). Polarized light imaging revealed increased collagen deposition and organization at 8 wk compared with 4 wk (Fig. 2G and K, arrows). IF analyses of Vimentin (VM)–expressing (green) mesenchymal cells and CD31-expressing endothelial cells showed increased organized neovascular formation over in vivo implantation time (Fig. 2D, H, L, arrows, and Appendix Movie 1).

(G2) Acellular GelMA-Filled Tooth RSs

G2 constructs exhibited acellular GelMA after 13 d of in vitro culture (Fig. 3A–C). The 4-wk in vivo implanted G2 constructs exhibited host cell infiltration and attachment to GelMA (Fig. 3D–F). Host cell density and attachment to GelMA appeared to increase in 8-wk in vivo implanted constructs (Fig. 3H–J). Host red blood cells were evident in 4-wk and 8-wk G2 constructs (Fig. 3E, I, arrows). Polarized light microscopy revealed increased host cell collagen deposition and organization in 8-wk constructs compared with 4-wk constructs (Fig. 3F, J, gold arrows). Double IF revealed VM-expressing host mesenchymal (green) and CD31-expressing host endothelial cells (red) in 4-wk and 8-wk constructs and organized neovasculature formation in 8-wk in vivo implanted constructs (Fig. 3G, K, arrows, and Appendix Movie 2).

(G3) Empty Tooth RSs

In vivo implanted G3 constructs exhibited host cell infiltration at 4 wk and 8 wk (Fig. 4A, B and 4E, F, respectively). Host cell–derived extracellular matrix (ECM) in implanted G3 constructs appeared more organized in 8-wk constructs compared with 4-wk constructs, as revealed by polarized light

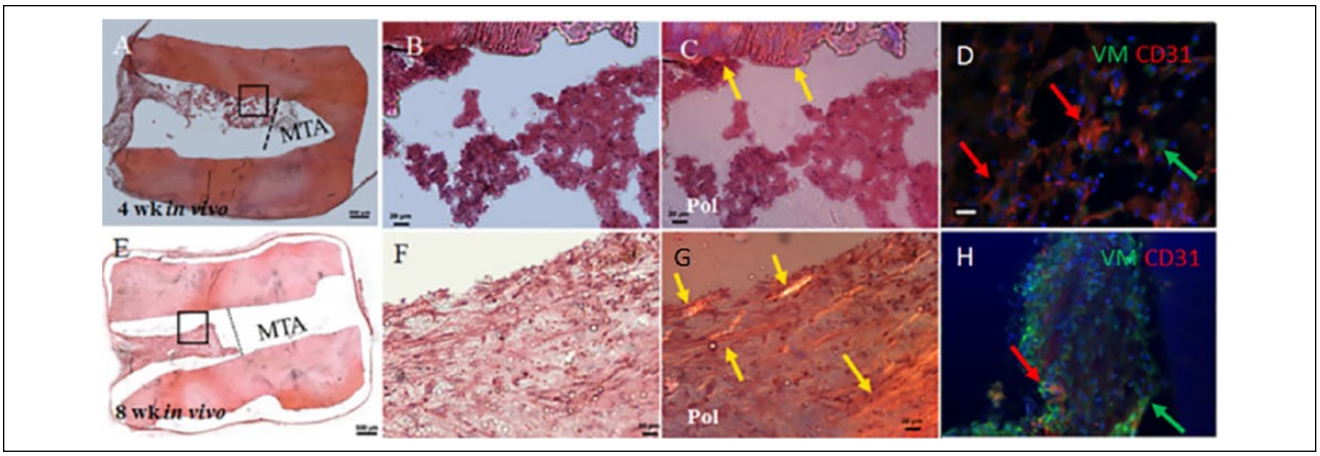

Figure 4. Empty root segment (RS) constructs (G3). (**A**) G3 constructs at 4 wk of in vivo implantation showed host cell infiltration into the pulpal space. (**B**) Enlarged view of boxed area in A showing host cell infiltration into the pulpal space. (**C**) Polarized light revealed dentin extracellular matrix (ECM) only (yellow arrows). (**D**) Double immunofluorescence (IF) revealed the presence of host endothelial and mesenchymal tissues at 4 wk of implantation. (**E**) The 8-wk in vivo implanted G3 constructs exhibited increased cellularity compared with 4-wk G3 implants. (**F**) More distinct host cellularity was observed in 8-wk compared with 4-wk in vivo implanted G3 samples. (**G**) Polarized light imaging revealed increased host ECM deposition at 8-wk compared with 4-wk in vivo implantation (yellow arrow). (**H**) Double IF showed similar results as the 4-wk in vivo implanted G3 constructs. Scale bars: A, E = 500 μm; B, F, C, G = 20 μm; and D, H = 50 μm. This figure is available in color online.

microscopy (Fig. 4G versus C). IF histochemical analyses revealed CD31 (red)–positive host endothelial cells in 4-wk implants and both CD31-positive endothelial cells and VM (green)–expressing mesenchymal stem cells (MSCs) in 8-wk in vivo implants (Fig. 4D, H, arrows, and Appendix Movie 3). Neovasculature formation in empty RSs appeared less organized that that observed in acellular G2 constructs and much less than was observed in the in vivo implanted G1 constructs. Negative control IFs are shown in Appendix Figure 1.

High-Magnification Imaging of G1, G2, and G3 Constructs

High-magnification imaging was used to compare bioengineered pulp formation in the center, as well as cell interactions at the inner dentin surface, of implanted tooth root constructs. The G1 GelMA-encapsulated hDPC/HUVEC constructs exhibited highly cellularized pulp centers after 13 d of in vitro culture (week 0) (Fig. 5A). As expected, week 0 G2 acellular GelMA constructs showed GelMA scaffold with no cells, and week 0 empty segments were empty (Fig. 5A). After 4-wk in vivo implantation, the bioengineered pulp of the G1 constructs appeared highly cellularized and vascularized, with patent blood vessels and host red blood cells visible (Fig. 5A, arrows). The 4-wk G2, acellular GelMA constructs also exhibited some cellularity at the pulp center but much reduced compared with the G1 constructs, with no patent blood vessels and only a few RBCs identifiable (Fig. 5A, arrow). The 4-wk G3, empty root segment constructs exhibited pulp centers consisting of disorganized host cell infiltration with no organized vasculature (Fig. 5A). After 8 wk of implantation, the G1 constructs exhibited highly organized, patent vasculature carrying host RBCs. In contrast, 8-wk implanted G2 constructs exhibited few patent vessels, and similarly, 8-wk implanted G3 constructs exhibited disorganized pulp with immature vasculature (Fig. 5A).

We next looked for evidence of cell interactions with the inner dentin surface in each type of tooth root construct. The G1 constructs exhibited GelMA and cell attachment to the inner dentin surface at week 0, week 4, and week 8. As shown by H&E staining and polarized light microscopy, cell attachment to the inner dentin surface increased with longer implantation times, and the attached cells also exhibited increased numbers and lengths of cellular extensions into the dentin tubules (Fig. 5B). Polarized light imaging revealed that increased matrix deposition was evident at 8-wk compared with 4-wk constructs, indicative of initial stages of reparative dentin secretion (Fig. 5B). G2, acellular GelMA constructs showed GelMA attachment to the inner dentin surface at week 0. At 4 wk of implantation, G2 constructs exhibited thin threads of GelMA attachment, while none were observed in 8-wk implanted constructs. G3, empty tooth RS did not exhibit host cell attachment to the inner dentin surface in any of the replicate week 0, week 4, or week 8 constructs.

Discriminating between GelMA Encapsulated Human (G1) and Rat Host Cells

To evaluate the long-term survival of GelMA-encapsulated human DPSC/HUVEC cells and to discriminate between human and host cells, sectioned samples were examined via IF using an anti–rh-mitochondria antibody that recognizes human cells and does not cross-react with rat cells (Popescu et al. 2013). Human mitochondrial expressing human DPSC/HUVECs were identifiable in G1 constructs at 13 d of in vitro culture and after 4-wk of in vivo implantation (Appendix Fig. 2A, B, arrows). Human cells were not detectable in the 8-wk G1 constructs (Appendix Fig. 2C). G2 and G3 constructs exhibited no positive rh-mitochondria expression (Appendix Fig. 2D, E, G, H). Human gingiva was positive for rh-mitochondria (Appendix Fig. 2F). Quantification of the rh-mitochondria–positive cells showed

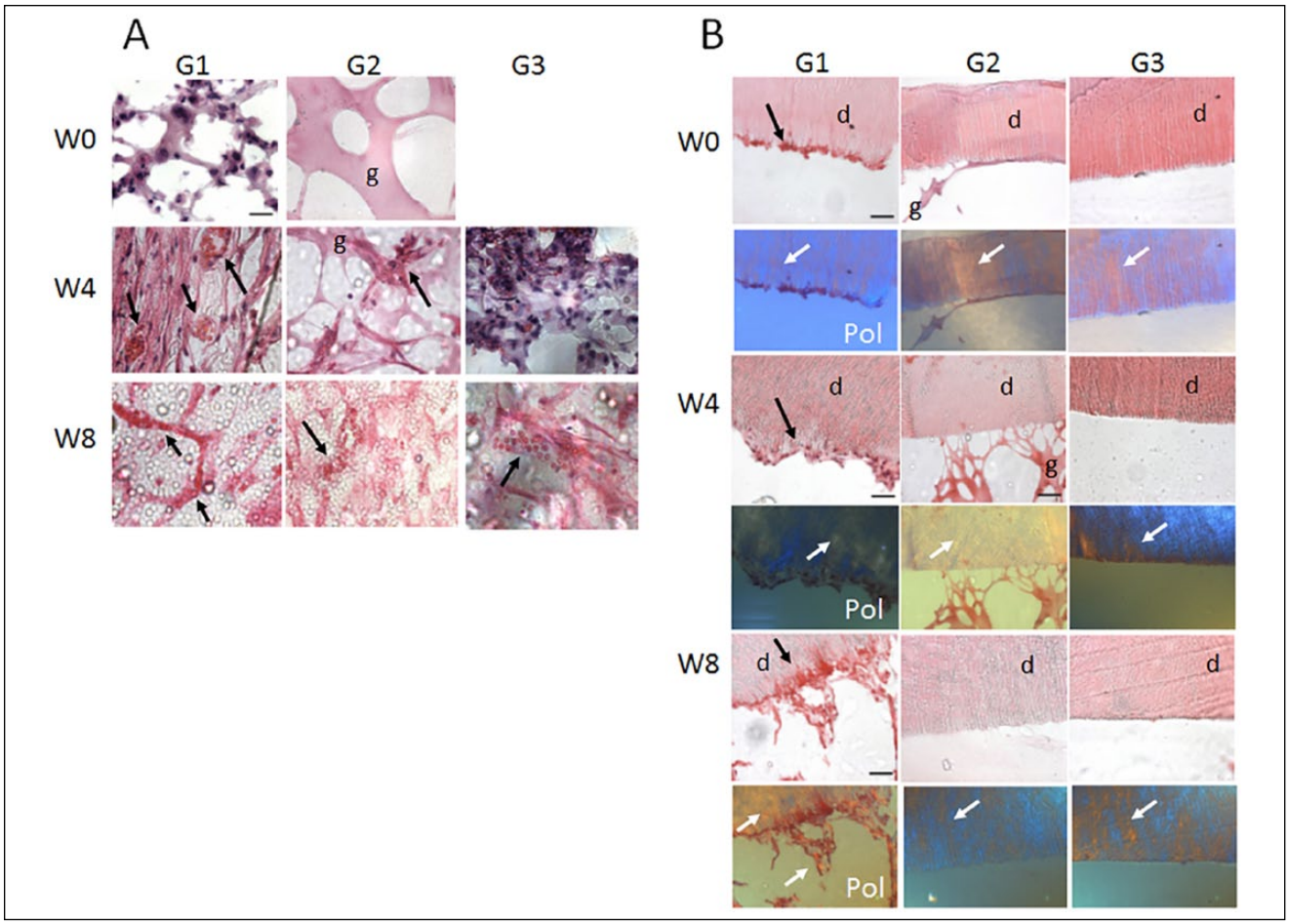

Figure 5. Bioengineered dental pulp vascularization and interactions with inner dentin surface. (**A**) High-magnification images of the pulp center of representative in vivo implanted G1, G2, and G3 constructs. G1, human dental pulp stem cell (hDPSC)/human umbilical vein endothelial cell (HUVEC)–encapsulated gelatin methacrylate (GelMA) constructs exhibited high cellularity at week 0, as well as increased cellularity and host red blood cell (RBC) circulation at 4 and 8 wk. G2 acellular GelMA samples exhibited a degree of host cell infiltration at 4 wk and disorganized vasculature formation at 8 wk of implantation. G3, empty tooth root segment (RS) exhibited some host cell infiltration at 2 wk and less well-organized host blood vessel formation at 8 wk compared with G2 constructs. (**B**) The inner dentin surface of G1, hDPSC/HUVEC-encapsulated GelMA constructs showed hDPSC/HUVEC cell attachment after 1 wk of in vitro culture (week 0) and increased cell attachment over in vivo implantation time (week 4, week 8). Polarized light imaging revealed increased collagen deposition and organization at the inner dentin surface over in vivo implantation time and increased formation and length of cellular extensions into the dentin tubules, indicative of reparative dentin formation and tooth revitalization. G2, acellular tooth root constructs showed GelMA attachment at week 0 and week 4 but no remaining GelMA present at week 8. Although host cells infiltrated into acellular GelMA construct pulp centers, no host cell attachment to inner dentin surface was observed in these constructs. Similarly, G3, empty tooth RSs did not show cell attachment to inner dentin surface at any of the times investigated.

~60% human cells present in 4-wk constructs and ~10% human cells present in 8-wk implanted G1 constructs (Appendix Fig. 3).

We also performed quantification of combined human and host cell contributions to implanted constructs over time. These results showed a fairly constant number of $CD31^+$ endothelial cells within the implants over the 8-wk implantation time, and an increase in $vimentin^+$ cells in G1, G2, and G3 constructs over in vivo implantation time (Appendix Fig. 4). Combined with the Appendix Figure 2 data, these results show the gradual replacement of human implanted hDPSC/HUVECs with host mesenchymal and endothelial cells over in vivo implantation time.

Remnant WMTA, used to seal off one end of each RS to mimic clinical treatment of a natural tooth, is clearly identifiable in sectioned implants (Figs. 2–4). We did not observe reparative dentin formation below the MTA, as previously reported, possibly due to the relatively short duration of our in vivo study (1–2 mo compared with 3–4 mo) (Huang et al. 2010; Parirokh et al. 2011; Schneider et al. 2014).

Discussion

The goal of our study was to define a more effective, clinically relevant method for pulpal revascularization and regeneration in human tooth RSs. A few recent studies report the use of hDPSCs for pulpal regeneration, showing that DPSCs can regenerate dentin-pulp complex when seeded onto poly-D,L-lactide/glycolide scaffolds and implanted in vivo for 3 to 4 mo

(Huang et al. 2010) and the use of peptide hydrogels for pulp regeneration (Dissanayaka et al. 2014). Despite these promising reports, current challenges include identifying a scaffold that truly mimics the ECM of natural pulp and creating sufficient blood supply, in a timely manner, to ensure the survival of in vivo transplanted DPSCs and/or efficient recruitment of host cells to revitalize the tooth (Dissanayaka et al. 2014).

We chose to use both hDPSCs and HUVECs in our model, based on the importance of both types of cells for pulp tissue formation and vascularity (Nait Lechguer et al. 2008). hDPSCs are highly proliferative and exhibit the ability for self-renewal and the ability to form odontoblast-like cells, pulp-like tissues, reparative dentin, and bone-like tissue (Gronthos et al. 2000). In vitro studies demonstrated the ability of hDPSCs to differentiate into odontoblasts capable of forming mineralized nodules and polarized cell bodies (Tsukamoto et al. 1992; About et al. 2000; Couble et al. 2000).

Prior reports also showed that DPSCs play an important role in angiogenesis when combined with HUVECs by enhancing HUVEC migration and VEGF secretion, as well as promoting ECM deposition and mineralization (Dissanayaka et al. 2014). A functional vascularized network is essential for the long-term survival of bioengineered tissues and for proper integration with the recipient host (Novosel et al. 2011). Published reports showed that MSCs, including hDPSCs, and endothelial cells can self-organize into capillary-like networks after encapsulation in GelMA hydrogel in vitro and in vivo (Huang et al. 2010; Chen, Lin, et al. 2012; Smith et al. 2016). Based on these reports, we chose to use both cell types—hDPSCs and HUVECs—to promote bioengineered pulp neovasculature formation and host cell infiltration, attachment, and proliferation. hDPCs may also elicit an immunomodulatory response through the secretion of bioactive soluble factors that are conducive to host cell infiltration and tissue regeneration (De Miguel et al. 2012; Racz et al. 2014; Liu et al. 2015; Ozdemir et al. 2016). Consistent with prior reports, we did not observe any inflammation at our implant sites or the presence of inflammatory cells in any of our harvested and sectioned implants.

We chose to encapsulate hDPSCs and HUVECs in GelMA hydrogels, a preferred hydrogel scaffold for 3D tissue engineering applications based on its ability to facilitate cell attachment, spreading, proliferation, and promotion of host cell interactions (Nichol et al. 2010; Hosseini et al. 2012). The ability to easily inject and photo-crosslink GelMA encapsulated cells also makes GelMA an attractive scaffold for clinically relevant pulpal regeneration procedures. Our recently published reports characterizing bioengineered 3D tooth buds created from GelMA-encapsulated DE and DM cell layers showed superb biocompatibility and cell proliferation (Smith et al. 2014; Smith et al. 2016). The goal of that study was to promote DE/HUVEC and DM/HUVEC cell layer interactions in a biomimetic 3D tooth bud model.

In contrast, the novelty in the study described here is the use of GelMA hydrogels for applications in pulp regeneration therapies. Our results showed that GelMA-encapsulated hDPSC/HUVECs contributed to the formation of bioengineered pulp-like tissue that exhibited increased cellularity increased over in vivo implantation time (Fig. 2). Furthermore, GelMA-encapsulated hDPSC/HUVECs contributed to the formation of organized and functional vasculature within highly cellularized pulp centers. GelMA hDPSC/HUVEC constructs also exhibited cell attachment to the inner dentin surface, the formation of cellular extensions into dentin tubules of the human tooth root segment, and increased matrix deposition at the tooth root inner dentin layer. All of these results indicate revitalization of the tooth RS in G1 constructs. In comparison, acellular GelMA and empty tooth root constructs did not exhibit any host cell attachment to dentin surface and reduced formation of organized neovasculature.

IF analyses using rh-mitochondria showed that the GelMA-encapsulated hDPSCs and HUVECs were detectable in 4-wk in vivo implants but not in 8-wk constructs (Appendix Fig. 2D). These results are consistent with published reports that implanted cells may not survive over the long term (Yates et al. 2016). Implanted cells can migrate from implanted constructs into the surrounding tissues (Gaudet et al. 2015) or can be eliminated by the host, although in our study, no inflammatory response was observed at the implant site or in harvested implants. It is likely that the regenerative effects of human cell seeded GelMA constructs contributed to host cell invasion and long-term establishment of cellularized pulp and patent vasculature. Consistent with this conclusion, G1 constructs exhibited cellularized pulp, cell attachment to the inner dentin surface, and elaboration of matrix and cell invasion into dentin tubules of all replicate constructs. In contrast, G2 acellular GelMA and G3 empty tooth root constructs exhibited a lesser degree of host cell infiltration into the pulp chamber and no host cell attachment to the inner dentin surface.

Conclusion

In conclusion, our results demonstrate that GelMA hydrogels can support the formation of highly cellularized and vascularized hDPC/HUVEC-derived pulp like tissue in in vivo implanted human tooth RSs, facilitate attachment of cells to the tooth root inner dentin surface, and promote the formation of cellular extensions into the dentin tubules and elaboration of reparative dentin matrix formation. In contrast, acellular GelMA and empty tooth root constructs exhibited host cell infiltration into the pulp chamber but no host cell attachment to the tooth root inner dentin surface. Together, these results validate GelMA-encapsulated hDPSC/HUVEC constructs as a promising therapy for pulpal revascularization, as an alternative to currently used devitalized tooth endodontic treatments.

Author Contributions

A. Khayat, contributed to conception, design, data acquisition, analysis, and interpretation, drafted and critically revised the manuscript; N. Monteiro, E. Smith, contributed to design, data acquisition, analysis, and interpretation, critically revised the manuscript; W. Zhang, S. Pagni, P.C. Yelick, contributed to design, data analysis, and interpretation, critically revised the manuscript; A.

Khademhosseini, contributed to design and data acquisition, critically revised the manuscript. All authors gave final approval and agree to be accountable for all aspects of the work.

Acknowledgments

This project was supported by National Institutes of Health/National Institute of Dental and Craniofacial Research RO1DE016132 (PCY), the Tufts University School of Dental Medicine Masters Project, and Tufts Center for Neuroscience Research, P30 NS047243 (Jackson). We acknowledge the expert technical assistance of Shantel Angstadt and Matthew Manning and the entire Yelick Laboratory for their support and guidance. The authors declare no potential conflicts of interest with respect to the authorship and/or publication of this article.

References

About I, Bottero MJ, de Denato P, Camps J, Franquin JC, Mitsiadis TA. 2000. Human dentin production in vitro. Exp Cell Res. 258(1):33–41.

Bansal R, Jain A, Mittal S, Kumar T, Kaur D. 2014. Regenerative endodontics: a road less travelled. J Clin Diagn Res. 8(10):ZE20–ZE24.

Chen MY, Chen KL, Chen CA, Tayebaty F, Rosenberg PA, Lin LM. 2012. Responses of immature permanent teeth with infected necrotic pulp tissue and apical periodontitis/abscess to revascularization procedures. Int Endod J. 45(3):294–305.

Chen YC, Lin RZ, Qi H, Yang Y, Bae H, Melero-Martin JM, Khademhosseini A. 2012. Functional human vascular network generated in photocrosslinkable gelatin methacrylate hydrogels. Adv Funct Mater. 22(10):2027–2039.

Chueh LH, Ho YC, Kuo TC, Lai WH, Chen YH, Chiang CP. 2009. Regenerative endodontic treatment for necrotic immature permanent teeth. J Endod. 35(2):160–164.

Cordeiro MM, Dong Z, Kaneko T, Zhang Z, Miyazawa M, Shi S, Smith AJ, Nor JE. 2008. Dental pulp tissue engineering with stem cells from exfoliated deciduous teeth. J Endod. 34(8):962–969.

Couble ML, Farges JC, Bleicher F, Perrat-Mabillon B, Boudeulle M, Magloire H. 2000. Odontoblast differentiation of human dental pulp cells in explant cultures. Calcif Tissue Int. 66(2):129–138.

De Miguel MP, Fuentes-Julian S, Blazquez-Martinez A, Pascual CY, Aller MA, Arias J, Arnalich-Montiel F. 2012. Immunosuppressive properties of mesenchymal stem cells: advances and applications. Curr Mol Med. 12(5):574–591.

Dissanayaka WL, Hargreaves KM, Jin L, Samaranayake LP, Zhang C. 2015. The interplay of dental pulp stem cells and endothelial cells in an injectable peptide hydrogel on angiogenesis and pulp regeneration in vivo. Tissue Eng Part A. 21(3–4):550–563.

Dissanayaka WL, Zhu L, Hargreaves KM, Jin L, Zhang C. 2014. Scaffold-free prevascularized microtissue spheroids for pulp regeneration. J Dent Res. 93(12):1296–1303.

Dissanayaka WL, Zhu L, Hargreaves KM, Jin L, Zhang C. 2015. In vitro analysis of scaffold-free prevascularized microtissue spheroids containing human dental pulp cells and endothelial cells. J Endod. 41(5):663–670.

Galler KM, D'Souza RN, Federlin M, Cavender AC, Hartgerink JD, Hecker S, Schmalz G. 2011. Dentin conditioning codetermines cell fate in regenerative endodontics. J Endod. 37(11):1536–1541.

Gaudet JM, Ribot EJ, Chen Y, Gilbert KM, Foster PJ. 2015. Tracking the fate of stem cell implants with fluorine-19 MRI. PLoS One. 10(3):e0118544.

Gronthos S, Mankani M, Brahim J, Robey PG, Shi S. 2000. Postnatal human dental pulp stem cells (DPSCs) in vitro and in vivo. Proc Natl Acad Sci U S A. 97(25):13625–13630.

Guo T, Li Y, Cao G, Zhang Z, Chang S, Czajka-Jakubowska A, Nor JE, Clarkson BH, Liu J. 2014. Fluorapatite-modified scaffold on dental pulp stem cell mineralization. J Dent Res. 93(12):1290–1295.

Hosseini V, Ahadian S, Ostrovidov S, Camci-Unal G, Chen S, Kaji H, Ramalingam M, Khademhosseini A. 2012. Engineered contractile skeletal muscle tissue on a microgrooved methacrylated gelatin substrate. Tissue Eng Part A. 18(23–24):2453–2465.

Huang GT, Yamaza T, Shea LD, Djouad F, Kuhn NZ, Tuan RS, Shi S. 2010. Stem/progenitor cell-mediated de novo regeneration of dental pulp with newly deposited continuous layer of dentin in an in vivo model. Tissue Eng Part A. 16(2):605–615.

Liu J, Yu F, Sun Y, Jiang B, Zhang W, Yang J, Xu GT, Liang A, Liu S. 2015. Concise reviews: characteristics and potential applications of human dental tissue-derived mesenchymal stem cells. Stem Cells. 33(3):627–638.

Nait Lechguer A, Kuchler-Bopp S, Hu B, Haikel Y, Lesot H. 2008. Vascularization of engineered teeth. J Dent Res. 87(12):1138–1143.

Nichol JW, Koshy ST, Bae H, Hwang CM, Yamanlar S, Khademhosseini A. 2010. Cell-laden microengineered gelatin methacrylate hydrogels. Biomaterials. 31(21):5536–5544.

Novosel EC, Kleinhans C, Kluger PJ. 2011. Vascularization is the key challenge in tissue engineering. Adv Drug Deliv Rev. 63(4–5):300–311.

Ozdemir AT, Ozgul Ozdemir RB, Kirmaz C, Sariboyaci AE, Unal Halbutogllari ZS, Ozel C, Karaoz E. 2016. The paracrine immunomodulatory interactions between the human dental pulp derived mesenchymal stem cells and CD4 T cell subsets. Cell Immunol. 310:108–115.

Palasuk J, Kamocki K, Hippenmeyer L, Platt JA, Spolnik KJ, Gregory RL, Bottino MC. 2014. Bimix antimicrobial scaffolds for regenerative endodontics. J Endod. 40(11):1879–1884.

Parirokh M, Asgary S, Eghbal MJ, Kakoei S, Samiee M. 2011. A comparative study of using a combination of calcium chloride and mineral trioxide aggregate as the pulp-capping agent on dogs' teeth. J Endod. 37(6):786–788.

Popescu IR, Nicaise C, Liu S, Bisch G, Knippenberg S, Daubie V, Bohl D, Pochet R. 2013. Neural progenitors derived from human induced pluripotent stem cells survive and differentiate upon transplantation into a rat model of amyotrophic lateral sclerosis. Stem Cells Transl Med. 2(3):167–174.

Qu T, Liu X. 2013. Nano-structured gelatin/bioactive glass hybrid scaffolds for the enhancement of odontogenic differentiation of human dental pulp stem cells. J Mater Chem B Mater Biol Med. 1(37):4764–4772.

Racz GZ, Kadar K, Foldes A, Kallo K, Perczel-Kovach K, Keremi B, Nagy A, Varga G. 2014. Immunomodulatory and potential therapeutic role of mesenchymal stem cells in periodontitis. J Physiol Pharmacol. 65(3):327–339.

Rosa V, Zhang Z, Grande RH, Nör JE. 2013. Dental pulp tissue engineering in full-length human root canals. J Dent Res. 92(11):970–975.

Schneider R, Holland GR, Chiego D Jr, Hu JC, Nör JE, Botero TM. 2014. White mineral trioxide aggregate induces migration and proliferation of stem cells from the apical papilla. J Endod. 40(7):931–936.

Shah N, Logani A, Bhaskar U, Aggarwal V. 2008. Efficacy of revascularization to induce apexification/apexogensis in infected, nonvital, immature teeth: a pilot clinical study. J Endod. 34(8):919–925; discussion 1157.

Smith EE, Yelick PC, Khademhosseini A. 2014. Optimization of a biomimetic model for tooth regeneration. Proceedings 2014 40th Annual Northeast Bioengineering Conference (NEBEC), 1–2 December. IEEE; Boston, MA.

Smith EE, Zhang W, Schiele NR, Khademhosseini A, Kuo CK, Yelick PC. 2016. Developing a biomimetic tooth bud model. J Tissue Eng Regen Med. In press. doi:10.1002/TERM.2246

Syed-Picard FN, Ray HL Jr, Kumta PN, Sfeir C. 2014. Scaffoldless tissue-engineered dental pulp cell constructs for endodontic therapy. J Dent Res. 93(3):250–255.

Tsukamoto Y, Fukutani S, Shin-Ike T, Kubota T, Sato S, Suzuki Y, Mori M. 1992. Mineralized nodule formation by cultures of human dental pulp-derived fibroblasts. Arch Oral Biol. 37(12):1045–1055.

Yates CC, Nuschke A, Rodrigues M, Whaley D, Dechant JJ, Taylor DP, Wells A. 2016. Improved transplanted stem cell survival in a polymer gel supplemented with tenascin-C accelerates healing and reduces scarring of murine skin wounds. Cell Transplant [epub ahead of print 22 Jul 2016] in press.

Zhang W, Ahluwalia IP, Yelick PC. 2010. Three dimensional dental epithelial-mesenchymal constructs of predetermined size and shape for tooth regeneration. Biomaterials. 31(31):7995–8003.

Zhang W, Zhang Z, Chen S, Macri L, Kohn J, Yelick PC. 2016. Mandibular jaw bone regeneration using human dental cell-seeded tyrosine-derived polycarbonate scaffolds. Tissue Eng Part A. 22(13–14):985–993.

Zhujiang A, Kim SG. 2016. Regenerative endodontic treatment of an immature necrotic molar with arrested root development by using recombinant human platelet-derived growth factor: a case report. J Endod. 42(1):72–75.